

## Processing of data with continuous source and receiver side wavefields - Real data examples

Tilman Klüver\* (PGS), Stian Hegna (PGS), and Jostein Lima (PGS)

### Summary

In this paper, we describe the processing steps to extract the response of the earth from data acquired using continuous source and receiver side wavefields. This will be demonstrated using real data examples. In a companion paper (Hegna et al., 2018, Benefits of continuous source and receiver side wavefields, abstract submitted to SEG Annual Meeting) we describe the methodology, outline differences to the conventional shot record based seismic method. The benefits in terms of improved efficiency, source side sampling and reduced environmental impact from less emitted sound is also discussed in that paper .

### Introduction

We introduced a novel seismic acquisition and processing methodology in a companion paper that uses continuous source and receiver side wavefields to extract the response of the earth, i.e. the data that would have been recorded due to a source emitting a band-limited spike. The method uses a continuous source wavefield which can be realized with existing equipment by triggering single air-guns in dense, randomized time intervals. The resulting continuous source wavefield approaches the properties of white noise. Data on the receiver side are treated continuously for typically the length of a sail-line. In the case of towed streamer data, the data are converted to stationary receiver positions by correcting for the streamer movement during acquisition. The source wavefields are deconvolved from traces in stationary receiver locations in an iterative fashion to extract common receiver gathers containing the response of the earth associated with each source in each receiver location.

In this paper, we detail the processing steps particular to this method and illustrate the processing results with field data examples. We first summarize all processing steps and then explain them in more detail.

### Method

The processing of data acquired with continuous source wavefields follows the flowchart shown in Figure 1. The first step in the processing sequence corrects for analogue filtering effects in the data. The different analogue filter responses of pressure and particle motion measurements in dual-sensor streamers are deconvolved from the data, and the particle motion recordings are converted to the pressure equivalent by scaling with the acoustic impedance at streamer depth.

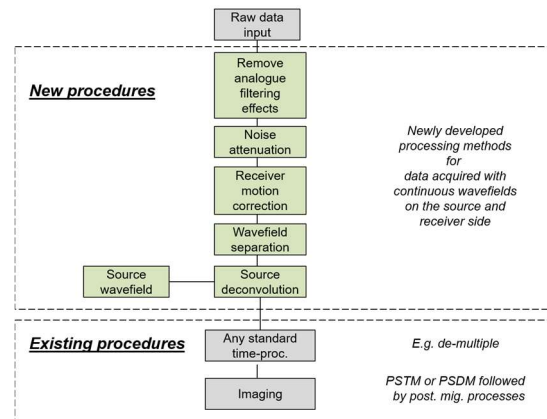


Figure 1: Processing flowchart. The continuously recorded input data go through several steps specific to the new methodology before processing continues with existing processing and imaging algorithms.

In the next step, pressure and particle motion measurements undergo noise attenuation. The methods used in this step are specifically designed to take advantage of the long record length when dealing with a continuous seismic record from one sail-line at once.

In the next step, the continuous motion of the streamers during acquisition is corrected for, which transforms the data in stationary positions along the moving streamer(s) into the corresponding data in stationary receiver locations.

The receiver motion correction is followed by wavefield separation: the pressure and particle motion data are combined to separate the recorded wavefield into up-going and down-going parts.

The last step before continuing with conventional processing is the deconvolution of the source wavefield. This step converts the data received in each stationary receiver location into common receiver gathers, one for each source being operated simultaneously, containing the response of the earth, i.e. the wavefield that would have been recorded with point sources emitting a band-limited spike.

### Noise attenuation

We have developed noise attenuation methods that take advantage of the long records when working with data from a complete sail-line. These records are typically several hours long.

## Processing of data with continuous wavefields

The particle motion data is typically noisier towards the low frequency end of the spectrum than the pressure data. We utilize having two recordings of the same signal, one of which is cleaner than the other one, to significantly attenuate noise on the particle motion data. Differences in analogue filter responses have been corrected for in the first step of the processing flow visualized in Figure 1. The particle motion data has been converted to its pressure equivalent. The remaining signal differences, i.e. the difference between pressure and vertical particle velocity ghost functions and the obliquity correction, are removed by equalizing the two components using cross-ghosting:

$$P(\omega, k)(1 + e^{-ik_z 2z_r}) \frac{ck_z}{\omega} = V_z(\omega, k)(1 - e^{-ik_z 2z_r}), \quad (1)$$

where  $P$  and  $V_z$  are the pressure and vertical particle velocity data, respectively. Angular horizontal wavenumber is denoted  $k$ ,  $k_z$  is angular vertical wavenumber, and  $\omega$  is angular frequency. The receiver depth is given by  $z_r$ .

After equalizing both components, the cross-ghosted, clean pressure data is deconvolved from the cross-ghosted, noisy particle velocity data. The signal is thereby collapsed whereas the noise is spread out since it does not correlate with the signal. The longer the record the better the separation of signal and noise becomes. This is used to generate a model of the noise in the vertical particle velocity data. That noise model is then subtracted from the input data.

Figure 3 shows a comparison in the f-k domain of vertical particle velocity data before and after noise attenuation. Signal below 10 Hz is clearly visible after noise attenuation, which is completely obscured by low frequency noise in the input data.

### Receiver motion correction

The next step in the processing sequence is the receiver motion correction. The streamer data are transformed into stationary receiver traces with a spatial phase shift of the form

$$R_m(t, k) = R(t, k)e^{-ik\Delta x_r(t)}, \quad (2)$$

where  $R$  is the recorded data,  $R_m$  is the data after motion correction,  $t$  and  $k$  denote time and horizontal wavenumber with respect to the receiver coordinate, respectively, and  $\Delta x_r$  is the receiver motion. The density of stationary receiver traces regularly spaced along the sail-line is a processing parameter and is typically chosen equal to the channel spacing in the streamer. The live data length in each receiver trace is given by the time it takes to move the entire streamer length over the stationary receiver position. For an 8000 m

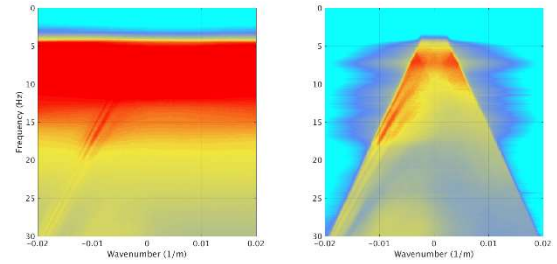


Figure 3: Input to (left) and output of (right) a novel noise attenuation method for particle motion data based on long continuous records. After noise attenuation signal can be identified to below 10 Hz which is completely obscured by noise in the input data. The colours cover a 60dB range from blue to red, and have the same dB scale in both spectra.

long streamer and an average bottom speed of 2.5 m/s, a receiver trace will contain about 3200 seconds of live data. Figure 4 shows data after receiver motion correction.

### Wavefield separation

The wavefield separation follows the methodology described by Carlson et al. (2007). It is, however, not applied shot record by shot record, but on the data of a full sailline after receiver motion correction, i.e. on data of the form shown on the right hand side of Figure 4. The up-going pressure is expressed in the frequency-wavenumber domain by

$$P_{up}(\omega, k) = \frac{1}{2} \left( P(\omega, k) - \frac{\omega}{ck_z} V_z(\omega, k) \right), \quad (3)$$

where all quantities are as in equation 1. The effect of the wavefield separation is illustrated in Figure 5.

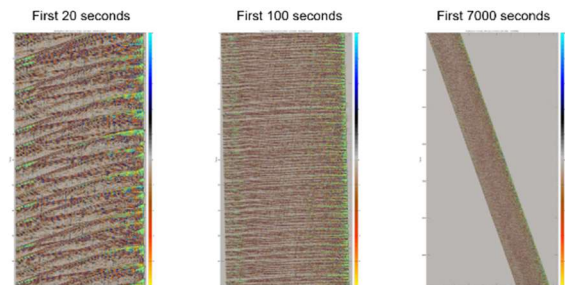


Figure 4: Data after receiver motion correction shown in three differently sized time windows. The window on the left shows 20 s of data, the center window shows 100s of data, and the window on the right shows the first 7000 s of data of the sailline.

## Processing of data with continuous wavefields

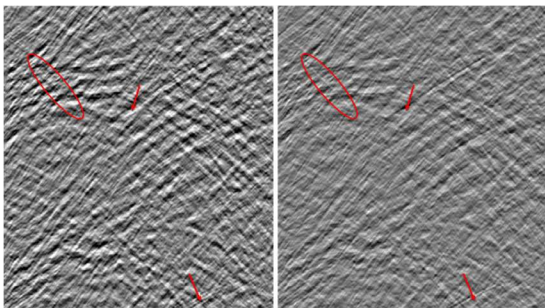


Figure 5: Recorded pressure data (left) and up-going pressure data (right) obtained by wavefield separation. The displayed window is 1 s long and 3500 m wide. Wavefield separation greatly simplifies the wavefield. The disappearing receiver side ghost reflection is marked in a few spots.

### Source deconvolution

In the final step, the source wavefields are deconvolved from each receiver trace converting each stationary receiver trace into receiver gathers, one for each source, containing the response of the earth. As described in the companion paper, the source deconvolution requires as an input the source wavefield(s) contributing to each receiver location generated by triggering individual air-guns with dense, randomized time intervals. The source wavefield is built from notional source signatures derived from near-field recordings as described by Ziolkowski et al. (1982). One individual notional per air-gun triggering is derived, which captures any variations in the emitted wavefields. Figure 6 shows notional signatures derived for a single air-gun from near-field measurements.

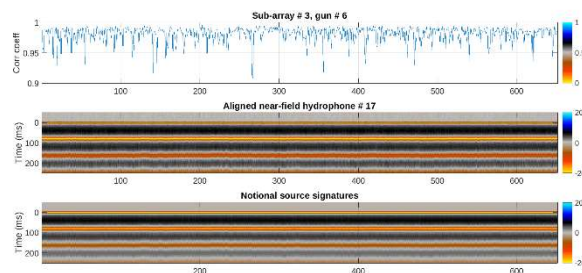


Figure 6: The graph on top shows the correlation coefficient between trimmed mean stacked near-field hydrophone data for a single gun and the near-field measurements of the individual firings for the same gun. The image in the middle shows the near-field hydrophone data from the hydrophone closest to the firing gun after aligning all the firings (correcting for the trigger times). The image at the bottom shows the final notional source signatures for each firing.

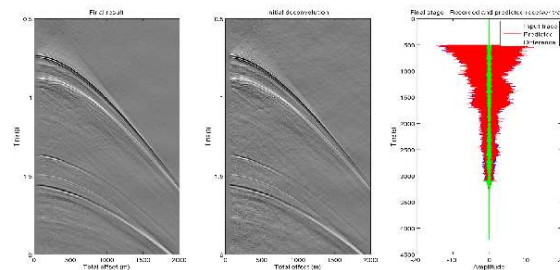


Figure 7: Initial deconvolution result (center) and final extracted earth response (left) of the iterative source deconvolution scheme. The right-hand figure shows the input stationary receiver trace in blue, the receiver trace modelled with the extracted coherent signal in red, and the final residual receiver trace in green.

As outlined in the companion paper, the source deconvolution is an iterative process. The energy is placed in all angles and the source wavefield is deconvolved. Coherent energy is extracted from the deconvolution result and its contribution to the receiver trace is modelled and subtracted to generate a residual receiver trace containing signals that have not yet been explained. The process starts again with deconvolving the source wavefield from the residual receiver trace. The explained signal is accumulated during the iterations. The amount of noise generated in the deconvolution decreases as more and more signal is explained. When no more coherent signal can be extracted, the residual deconvolution result is added in order not to lose any signal. Figure 7 shows an example of the iterative deconvolution result.

A marine seismic vessel is typically equipped with six strings with air-guns. When generating continuous wavefields by triggering individual air-guns, each string can be configured and operated to make the correlation between the wavefields emitted from the strings very low. Each string can be equipped with air-guns of different volumes. This guarantees complementary bubble pulses that mitigates instabilities in the deconvolution due to deep notches in the spectrum of the wavefield emitted from a single air-gun. The arrangement of the air-guns is different on each string which enhances the coding achieved by dense randomized trigger times. This minimizes the correlation between the source wavefields emitted from each string and allows us to extract six common receiver gathers with earth responses from each receiver trace through the iterative deconvolution method, as shown in Figure 8. The air-gun strings were deployed with a separation of 12.5m in this case. The data to the very right of Figure 8 shows the difference between the earth responses extracted for the outermost two sources. The difference

## Processing of data with continuous wavefields

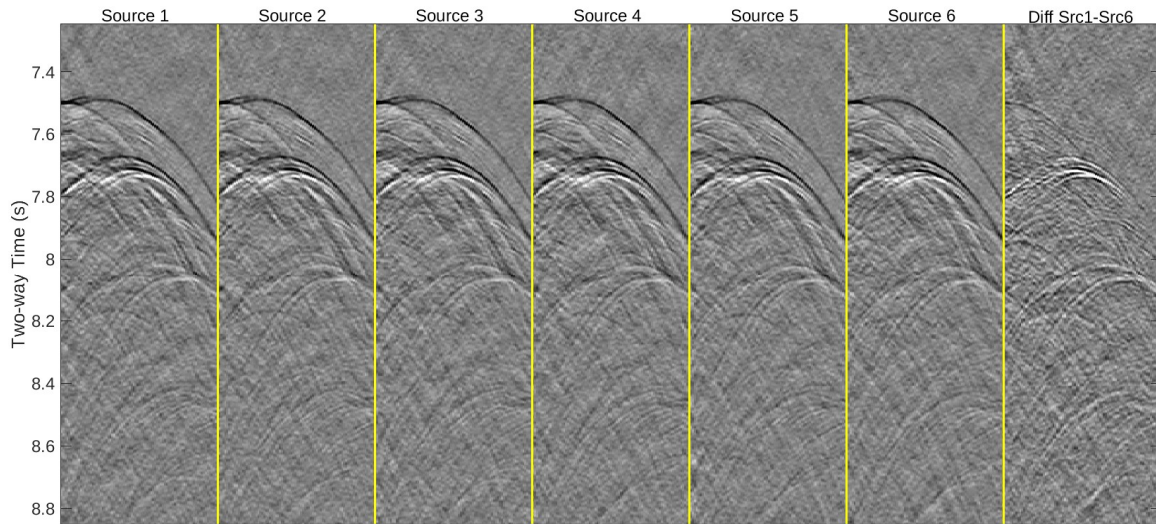


Figure 8: Example of extracting earth responses for a hexa-source configuration. The air-gun strings were spaced 12.5 m apart. The difference between the earth responses for the outermost two sources is shown on the right-hand side. The significant difference shows that a lot of the recorded signal has been emitted from the sources with a significant component in the crossline direction.

illustrates the variations in the extracted earth responses in the cross-line direction.

### Conclusions

We have discussed the processing steps with real data examples using a novel acquisition and processing method that utilizes continuous source and receiver side wavefields to extract the response of the earth from seismic data received in stationary receiver locations. The processing steps have been demonstrated using field data examples. The strong encoding of the continuous wavefield emitted from each source minimizes the correlation between the wavefields from several sources operated simultaneously. The effectiveness of extracting the response of the earth associated with each of the sources through an iterative source deconvolution approach has been shown for a configuration with six sources.

### Acknowledgments

We thank PGS for permission to publish this paper, and Statoil and The Research Council of Norway for funding the project together with PGS.

## REFERENCES

- Carlson, D., A. Long, W. Söllner, H. Tabti, R. TENGHAMN, and N. Lunde, 2007, Increased resolution and penetration from a towed dual sensor streamer. *First Break*, **25**, 71–77.
- Ziolkowski, A., G. E. Parkes, L. Hatton, and T. Haugland, 1982, The signature of an airgun array: Computation from near-field measurements including interactions — Part I: *Geophysics*, **47**, 1413–1421, <https://doi.org/10.1190/1.1441289>.